SILICATE-PEROVSKITE IN ACFER 040: A VERY HIGH SHOCK PRESSURE OF ONLY 26 GPA.

T. G. Sharp[1], R. Trickey[1], J. Hu[1], Z. Xie[2] and P. S. De Carli[3] [1]School of Earth and Space Exploration, Arizona State University, Tempe, AZ 85287, U.S.A. tom.sharp@asu.edu, [2]Nanjing University, Nanjing China, [3]SRI International, 333 Ravenwood Ave., Menlo Park, CA 94025

Introduction: The impact history of meteorite parent bodies can be extracted by using shock effects in meteorites to estimate shock pressures and durations. Highly shocked chondrites generally contain shock veins with associated high-pressure minerals that form by crystallization of the shock melt or by transformation of host-rock fragments entrained in the melt [1]. The crystallization assemblage can constrain shock pressure and the kinetics of transformation processes can be used to constrain the duration of the shock event [2-5]. Here we use the mineralogy and microstructures of high-pressure minerals in Acfer 040 to show that the the shock veins crystallized at pressure (~ 26 GPa) that is high relative to other highly shocked L6 chondrites but much lower than shock pressure predicted by previous shock classification schemes [6].

Background: Acfer 040 is a highly shocked S6 L5-6 chondrite with numerous melt veins and pockets. This sample was the first in which akimotoite and silicate perovskite were identified as products of melt-vein crystallization [7]. In that initial study, only a small amount of the melt-vein matrix was examined by TEM. The purpose of this study is to characterize the mineralogy and microstructures of a variety of shock veins in the sample to constrain shock-vein crystallization pressures and therefore shock pressure. In addition, we investigate the transformed host-rock fragments in the melt veins to understand transformation mechanisms and conditions.

Methods: We used polarized light microscopy (PLM) and Raman spectroscopy to survey the shock features, melt-vein textures and high-pressure mineralogy. Field-emission SEM was used to further investigate melt-vein mineralogy and transformation textures. The FIB was used to prepare sections for TEM analyses, which are underway.

Results: *Melt-vein matrix:* There are two distinct crystallization assemblages in the melt eins and pockets: 1) akimotoite + $(Mg,Fe)SiO_3$-perovskite + ringwoodite (Fig. 1), as described in [6] and 2) $(Mg,Fe)SiO_3$-perovskite + ringwoodite. The perovskite-ringwoodite assemblage is visible in PLM images as a finely-granular blue matrix. The akimotoite-bearing assemblage has 10-µm colorless laths of akimotoite.

Ringwoodite: Ringwoodite occurs as pure polycrystalline-aggregate grains within melt veins and as rims on olivines and lamellae in partially transformed olivine at the margins of melt veins. These partially transformed olivines have a distinctly brown color and a lamellar texture in PLM images. FESEM images and EDX analysis show that the ringwoodite rims are fayalite-rich (Fa_{46}) relative to Fayolite-poor (Fa_{24}) olivine cores (Fig. 2). Complex olivine-ringwoodite intergrowths occur just within those rims where the olvine is highly depleted in fayalite content.

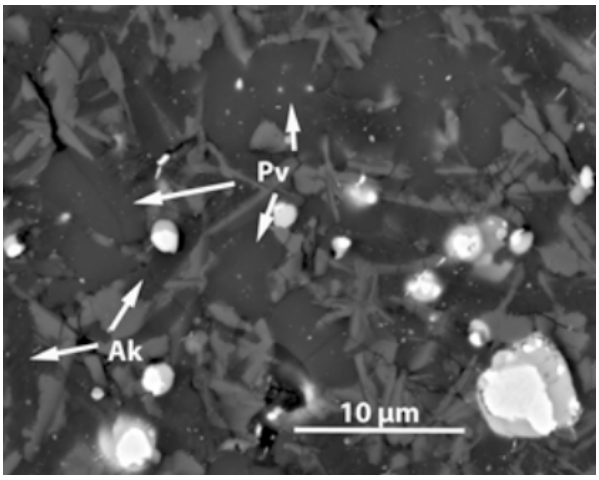

Fig. 1 BSE FESEM image of the melt-vein matrix with silicate perovskite (Pv), akimotoite (Ak) and ringwoodite.

$(Mg,Fe)SiO_3$-perovskite: Microstructures in BSE images suggest that enstatite is completely transformed to glass. Similarly, diopside grains in the melt veins are glassy. These observations suggest that both high- and low-Ca pyroxenes were transformed to silicate-perovskites or other unstable high-pressure phases that subsequently vitrified to glass during decompression. Most of the perovskite appears to have vitrified, but textures suggest that some crystalline perovskite remains in the sample. This is being confirmed with TEM.

Discussion: Partially transformed olivines have increasing ringwoodite contents toward melt veins, indicating that the olivine-ringwoodite transformation is driven by thermal heterogeneities during the shock-pressure pulse. The strong partitioning of fayalite component into the ringwoodite rims indicates that the transformation is diffusion controlled. This seems contrary to the timescales of the shock pulse, but it may indicate that either the transforming olivines were very

hot, or that localized deformation of the olivine has enhanced diffusion rates through pipe diffusion along dislocations. The role of deformation is supported by the complex textures of partially transformed olivine near the ringwoodite rims.

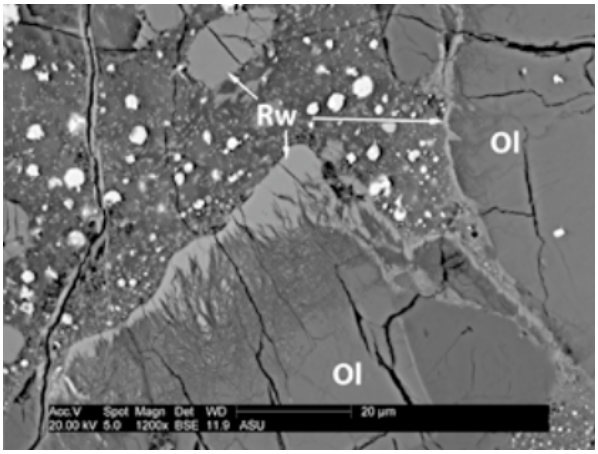

Fig. 2 Partially transformed olivine (Fa_{24}) with a rims of (Fa_{46}) ringwoodite at the margin of a shock-melt vein.

The fact that nearly all pyroxene-composition fragments in melt veins, both high- and low-Ca pyroxenes, are glassy indicates that the pyroxenes complete transformed to high-pressure polymorphs that vitrified during after pressure release. This vitrification is most likely in the thicker veins that remain hottest longest. In the thinner melt veins, textural evidence suggests that some of the pyroxene composition material retins the high-pressure structure. The most likely high-pressure polymorph is $(Mg,Fe)SiO_3$-perovskite.

Variations in melt-vein assemblage reflects variations in melt composition and quench history. The lack of majorite garnet and the ubiquity of vitrified $(Mg,Fe)SiO_3$-perovskite in the vein matrix assemblages indicates that the melt crystallized at a high pressure than most L6 S6 samples. Howver, the presence of silicate perovskite and ringwoodite in the assemblage suggests that the pressure was only marginally higher than in other highly shocked L6 chondrites. Although Acfer 040 may record the highest pressure melt-vein crystallization of any L6 chondrite, the crystallization pressure and therefore shock pressure is still much lower than estimates of S6 shock pressure based on the Stoffler et al classification [7].

References: [1] Chen, M. et al. (1996) *Science* 271, 1570-1573. [2] Sharp T. and De Carli P. (2006) *MESS II*, 653-677. [3] Xie, Z. et al. (2006) *GCA, 70.* 504-515. [4] Ohtani, E. et al. (2004) *EPSL 227(3-4),* 505-515. [5] Chen et al. (2004) *Proceedings. of NAS 101(42)*, 15033-15037. [6] D. Stöffler, et al., (1991) *GCA* 55, 3845. [7] Sharp et al. (1997) Science 277, 352-355.